

Short communication

Using numerical approximation as an intermediate step in analytical derivations: some observations from biomechanics

Zeike Taylor, Karol Miller*

Intelligent Systems for Medicine Laboratory, School of Mechanical Engineering, The University of Western Australia, 35 Stirling Highway, Crawley/Perth WA 6009, Australia

Accepted 12 October 2004

Abstract

We present four examples to illustrate the use of a type of numerical approximation as an intermediate step in analytical derivation of seemingly complicated biomechanical equations. The method involves examination of curve shapes to elucidate useful underlying trends, which may otherwise be overlooked through consideration of only the equations themselves. Two examples of the method's use are drawn from recently published results in the area of experimental methods in biomechanics of very soft tissues, and two others are taken from our current work on cartilage tissue mechanics. We think that such observations provide a useful means of circumventing complexity issues when deriving models for biomechanical analysis, and further that the method, while simple in concept, could be effective in a range of biomechanics applications.

© 2004 Elsevier Ltd. All rights reserved.

Keywords: Numerical approximation; Cartilage tissue; Very soft tissue; Viscoelasticity

1. Introduction

Investigations of a number of problems in tissue mechanics have yielded the useful observation that many apparently quite complicated relationships may be approximated by much simpler ones with virtually no loss of accuracy. This is achieved through scrutiny of the curve shapes (generated numerically in some cases) of such relations, and consideration of the true trend conveyed by these. While it may be desirable to retain exact equations, in many cases it is unnecessary, and possibly even prohibitive of further analytical development of the relevant biomechanical model. Such simplified relations can further be used in model development using analytical rather than numerical methods.

Four examples are presented in this paper to illustrate where use of such a process has proved valuable. Two of the examples draw on recent published research by members of the Intelligent Systems for Medicine Lab at the University of Western Australia (Miller, 2001, 2004), and two others are taken from our current work on cartilage tissue mechanics.

2. Example: analysis of extension and compression tests for soft tissues

Two examples of this process of numerical approximation based on observed curve shape may be drawn from recently published work on experimental methods for very soft tissue biomechanics. Miller (2001, 2004) presented analyses of two configurations for mechanical testing of very soft tissues: extension and compression of cylindrical samples with no-slip boundary conditions—top and bottom surfaces attached to opposing rigid plates, Fig. 1.

*Corresponding author. Tel.: +61 8 6488 7323;
fax: +61 8 6488 1024.

E-mail address: kmiller@mech.uwa.edu.au (K. Miller).

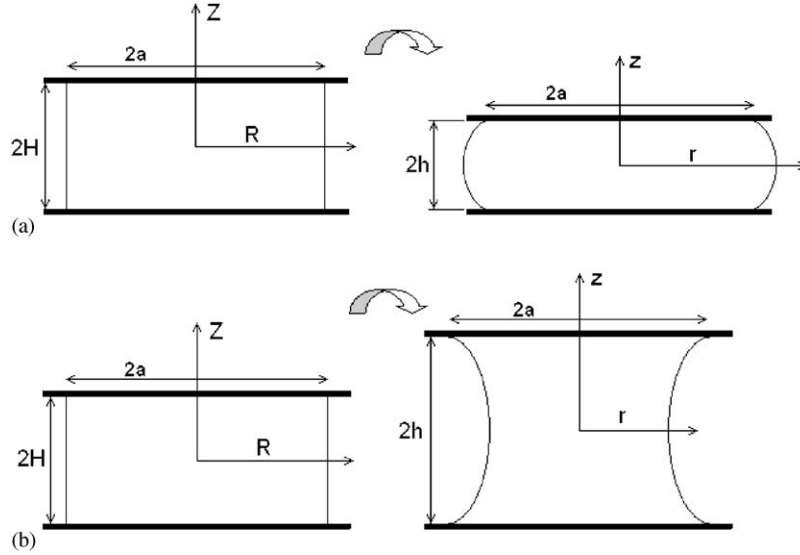


Fig. 1. Sketch of the experimental set-up with no-slip boundary conditions; (a) extension, (b) compression; the deformation is induced by the motion of the platens; sample height $2h$ and vertical force are measured.

In both cases it was of critical importance to relate the measured displacements of the load plates h/H and the vertical stretch in the plane of symmetry, $\lambda_z (Z = 0)$. For the extension case these relationships, assuming Neo-Hookean and Extreme-Mooney materials, are, respectively

$$\frac{h}{H} = \frac{\sqrt{1 - \lambda_z^{-1}}}{\lambda_z^{-1} \operatorname{arcsec} h(\lambda_z^{-1/2})}, \quad (1)$$

$$\frac{h}{H} = \frac{\arccos(\lambda_z^{-1/2})}{\lambda_z^{-1/2} \sqrt{1 - \lambda_z^{-1}}} \quad (2)$$

and for the compression case with similar respective material models

$$\frac{h}{H} = \frac{\sqrt{\lambda_z^2 - 1}}{\lambda_z^2 \operatorname{arcsec}(\lambda_z)}, \quad (3)$$

$$\frac{h}{H} = \frac{\arccos h(\lambda_z)}{\lambda_z \sqrt{\lambda_z^2 - 1}}. \quad (4)$$

These equations are sufficiently complicated that explicit expressions for the unknown stretch λ_z are unobtainable. While they may be solved numerically to obtain λ_z for a given displacement, h/H , they present a problem when considering investigation of *strain rate dependence* of the tissue. In such cases, one requires an indication of the stretch rate $\dot{\lambda}_z$ produced by a given velocity of the machine head, \dot{h}/H , and this is difficult to obtain from relations such as (1)–(4). A simpler solution based on the curve shape of Eqs. (1)–(4) was sought. Examination of such plots, Fig. 2, reveals that Eqs. (1)

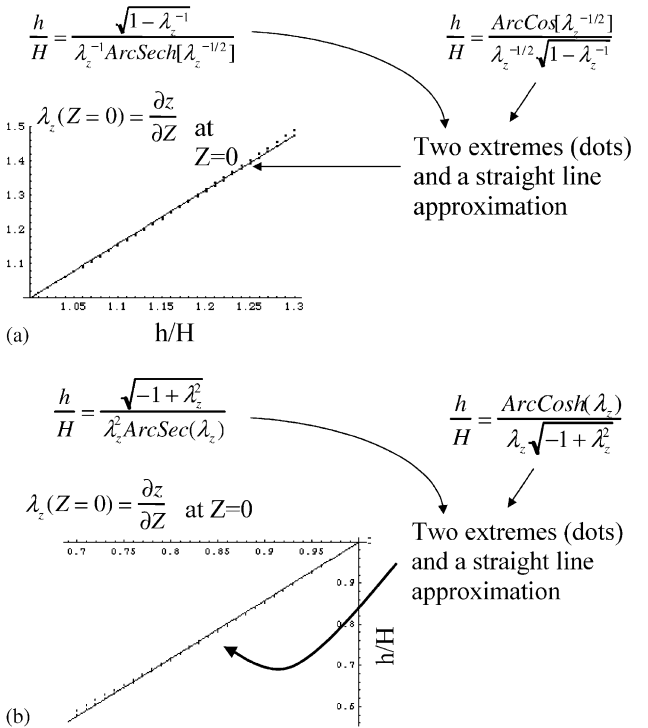


Fig. 2. Linear (for practical purposes) relationships between the measured machine head movement h/H and the vertical stretch in the plane of symmetry $\lambda_z (Z = 0)$ for samples made of Neo-Hookean and Extreme-Mooney materials. (a) extension, (b) compression (Miller, 2001, 2004).

and (2) (for extension) and (3) and (4) (for compression), respectively, approximate the same linear relationships to high level of accuracy, for stretch ratios up to $\sim 30\%$ (Miller, 2001, 2004). This is a very useful observation as

it implies that constant velocities of the machine head, \dot{h}/H , translate to constant stretch rates in the plane of symmetry, $\dot{\lambda}_z (Z=0)$ for extension

$$\dot{\lambda}_z (Z=0) = K \frac{\dot{h}}{H}; \quad K = 1.583, \quad (5)$$

for compression

$$\dot{\lambda}_z (Z=0) = K_c \frac{\dot{h}}{H}; \quad K_c = 1.411. \quad (6)$$

3. Example: viscoelastic fibre composite constitutive relations

An important topic of current interest in biomechanics is the development of relations between the macroscopic tissue mechanical response (called “effective characteristics” by composite materials community) and the tissue’s microstructure—particularly for the case of fibrous connective tissues. A number of efforts in this area have drawn on methods developed for analysis of fibre composite materials (Ault and Hoffman, 1992; Schwartz et al., 1994), and specifically the composite cylinders model of Hashin and Rosen (1964). This model is based on the concept of a fibrous material being composed of a large number of so-called fibre sub-units, which consist of a pair of coaxial cylinders. The inner and outer cylinders are assigned fibre and matrix material properties, respectively, and equations are derived for the effective properties of the composite. Such models can allow examination of the effects of variations in tissue constituent materials on the overall tissue mechanical response—that is, material properties of the tissue as a whole may be expressed as functions of the constituent material properties. The basic theoretical framework of the Hashin–Rosen model is well documented (Hashin and Rosen, 1964; Christensen and Waals, 1972; Ault and Hoffman, 1992), and so only the final result is stated here—that is, the overall tissue stiffness matrix, \bar{C}_{ij} , is obtained from the summation of responses of fibre sub-units oriented in all directions, weighted with an appropriate statistical fibre orientation distribution function, $f(\theta, \phi)$:

$$\bar{C}_{ij} = \int_0^{2\pi} \int_0^{\pi/2} f(\theta, \phi) C'_{ij} \sin \phi \, d\phi \, d\theta, \quad (7)$$

where C'_{ij} is the stiffness matrix (in global coordinates) of a fibre sub-unit with orientation given by the spherical coordinate angles θ and ϕ . One limitation of this model is that the constituent materials are taken to be linearly elastic, meaning that viscoelasticity is ignored completely, which for analysis of biological materials seems unacceptable. A possible solution to this problem is the incorporation of time-dependent con-

stituent material properties, for example, through the replacement of constant elastic parameters with so-called Prony series expansions of the form

$$\Omega(t) = \Omega_\infty + \sum_{i=1}^N \Omega_i e^{-t/\tau_i}, \quad (8)$$

where Ω_∞ represents the long-term modulus, Ω_i are relaxation moduli, and τ_i are relaxation times. If explicit relations can be obtained between the macroscopic and microscopic parameters, then direct substitution of equations of the form of (8) may be implemented. As will be seen though, such explicit relations are either complicated or unobtainable, and a process of numerical approximation is required.

The cases in point are the derivation of relations between the overall (effective) shear modulus of a fibrous connective tissue and the shear modulus of the tissue’s matrix phase using the Hashin–Rosen composite cylinders theory.

3.1. Case of uniform fibre orientation distribution

If we consider the case of a uniform distribution of fibre orientations, (7) may be evaluated directly and the result shown to be representative of an isotropic material (see Appendix A) (Christensen and Waals, 1972). From this follows a relation between the overall tissue shear modulus, \bar{G} , and the constituent matrix phase shear modulus, G_m :

$$\bar{G} = \frac{a_0 + a_1 G_m + a_2 G_m^2 + a_3 G_m^3 + a_4 G_m^4}{b_0 + b_1 G_m + b_2 G_m^2 + b_3 G_m^3}. \quad (9)$$

Coefficients a_0, \dots, a_4 and b_0, \dots, b_3 depend on properties of fibres G_f , v_f , matrix Poisson’s ratio v_m and the fibre volume fraction V_f . It should be noted that no common factors exist between the numerator and denominator polynomials of Eq. (9), meaning that no further algebraic simplification of the equation is possible. It thus appears that the relationship between \bar{G} and G_m is complicated; possibly strong nonlinearities exist close to the roots of the denominator, and incorporation of a time-dependent G_m of the form given in (8) would prove difficult. Inspection of a plot of Eq. (9) (Fig. 3), however, reveals that for a reasonable range of values of G_m (e.g. if we consider the case of articular cartilage, and treat the proteoglycan ground substance as constituting the matrix phase, then values up to 1 MPa may be considered reasonable—see e.g. Simha et al., 1999; Wilson et al., 2004, and references cited therein), the relationship is, for practical purposes, linear (linear fit correlation coefficient, $R > 0.999$).

The complicated expression in (9) may therefore be replaced with the significantly more tractable form:

$$\bar{G} \approx aG_m + b \quad (10)$$

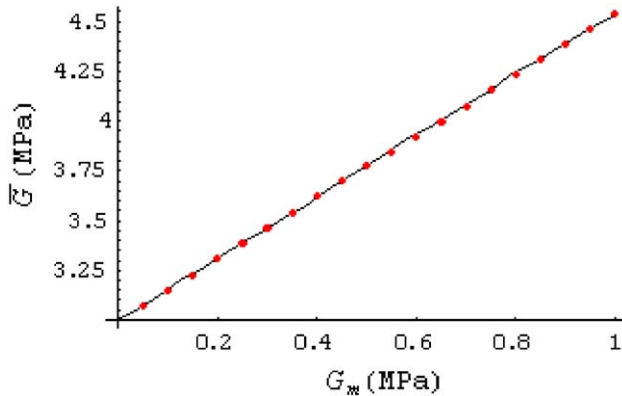


Fig. 3. Tissue overall shear modulus as a function of matrix phase shear modulus (●) using a spherical fibre orientation distribution, overlaid with a linear fit (—). Values for constituent material parameters are taken from Schwartz et al. (1994) for articular cartilage: $G_f = 53.57$ MPa (derived from Schwartz et al.'s Young's modulus and Poisson's ratio values of $E_f = 150$ MPa and $\nu_f = 0.4$, respectively, $G_f = E_f/2(1 + \nu_f)$), $\nu_f = 0.4$, $\nu_m = 0.3$, $V_f = 0.3$. The shear modulus of the proteoglycan matrix phase is assumed to lie in the range 0–1 MPa.

with virtually no loss of accuracy. Replacement of G_m with a time-dependent function is now a simple task, with a more availing result.

3.2. Case of ellipsoidal fibre orientation distribution

A further development of the previous example is the inclusion of an *ellipsoidal* fibre orientation distribution (as opposed to the *spherical* uniform case). This has the effect of introducing a degree of anisotropy to the distribution, and so is likely to better approximate *real* tissue fibre orientation distributions. For convenience, the semi-axes of the ellipsoid are taken to be aligned with the global coordinate axes (as defined in Ault and Hoffman, 1992). A spherical coordinate equation for the distribution is thus

$$f(\theta, \phi) = \frac{1}{\chi} \sqrt{\frac{1}{(\sin^2 \phi \cos^2 \theta/a^2) + (\sin^2 \phi \sin^2 \theta/b^2) + (\cos^2 \phi/c^2)}}, \quad (11)$$

where θ and ϕ are spherical coordinate angles. The square root term defines an ellipsoid with semi-axes lengths a , b , and c in the x -, y -, and z -directions, respectively. χ is a scaling factor for converting this arbitrary ellipsoid into a probability density function. Such a distribution may be shown to produce an orthotropic stiffness matrix. While there is no single overall (effective) shear modulus (\bar{G}) for the tissue in this case (in fact, there are three shear moduli, plus six other independent parameters), a relation between G_m and any of the overall stiffness matrix components (\bar{C}_{ij})

would still be very useful—i.e. we may seek a relation of the form $\bar{C}_{ij} = \Psi_{ij}(G_m)$. In this case, however, it proves prohibitively difficult to evaluate the double integral in (7) analytically, and so numerical integration must be used. This then raises the problem that G_m must take a numerical value, and an algebraic expression analogous to (9) cannot be found. In spite of this, a plot of a particular stiffness matrix component, $\bar{C}_{z\beta}$, versus G_m may still be obtained by evaluating Eq. (7) numerically for a range of G_m values. Such a plot is given for the case of \bar{C}_{11} in Fig. 4.

G_m is assigned values from 0 to 1 MPa in increments of 0.05, and other constituent material parameters are as used in the uniform distribution case. Again, it seems clear that a simple linear approximation may be used to a high level of accuracy (again, $R > 0.999$) for relating this component of the overall stiffness matrix to the constituent matrix phase shear modulus. A similar result may be obtained for each of the stiffness matrix components. As in the uniform distribution case explored above, this result is very useful for the further aim of incorporating a viscoelastic constitutive model for G_m . In particular, since in this case no explicit relation is obtainable from (7), examination of the form of the plot and use of numerical approximation is in fact a *necessary* step in the process.

It should be noted that in both the spherical and ellipsoidal cases, the stiffness matrices obtained in such a way may be directly implemented in a commercial finite element analysis package.

The obtained linearity of the relationship between the effective moduli $\bar{C}_{z\beta}$ and the matrix shear modulus G_m is not entirely unexpected because collagen fibres are treated as being two orders of magnitude stiffer than the matrix (for discussion see Germanovich

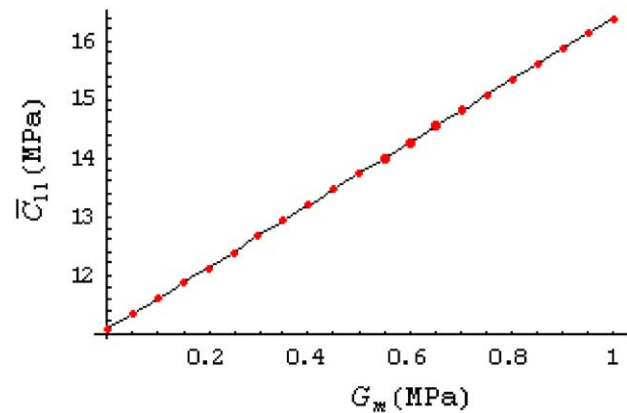


Fig. 4. Component (1,1) of the tissue overall stiffness matrix as a function of matrix phase shear modulus (●) using an ellipsoidal fibre orientation distribution, overlaid with a linear fit (—). \bar{C}_{11} is obtained by numerically integrating Eq. (7) for each value of G_m . Constituent material parameters are as used in the uniform distribution case, while ellipsoidal distribution semi-axes lengths are $a = 7$, $b = 5$, $c = 3$.

and Dyskin, 1994). However, for not too high fibre volume fractions ($V_f < 0.35$) this apparent linearity holds also for much lower G_f to G_m ratios, so that the linear relationship is not a limiting case valid only when $G_f/G_m \rightarrow \infty$.

It should be noted that this linearity is a feature of the mathematical model itself, and it will hold for real materials only in as much as the simplified assumptions behind Hashin–Rosen composite cylinders theory are satisfied.

4. Conclusions

Four examples from biomechanics illustrating the use of numerical approximation of seemingly complicated equations have been presented. Such observations are very useful from the point of view of further development of the respective models using

concept, could provide useful results in many areas of biomechanics.

Acknowledgements

The financial support of ARC SPIRT Grant (00107367), ARC Discovery Grant (DP0343112), and the UWA Grant is gratefully acknowledged. The authors would like to thank Prof. Arcady Dyskin for helpful discussions.

Appendix A. : Derivation of stiffness matrix and $\bar{G}-G_m$ relation for uniform fibre distribution

For a uniform distribution of fibres, there is no preferred direction, and so $f(\theta, \phi)$ becomes a constant ($= 1/2\pi$). Then,

$$\begin{aligned} \bar{C}_{ij} &= \int_0^{2\pi} \int_0^{\pi/2} f(\theta, \phi) C'_{ij} \sin \phi \, d\phi \, d\theta \\ &= \frac{1}{2\pi} \int_0^{2\pi} \int_0^{\pi/2} C'_{ij} \sin \phi \, d\phi \, d\theta \\ &= \frac{1}{30} \begin{bmatrix} 2(3C_{11} + 4C_{12} + 8C_{22} + 8C_{55}) & 2(C_{11} + 8C_{12} + C_{22} + 5C_{23} - 4C_{55}) & 2(C_{11} + 8C_{12} + C_{22} + 5C_{23} - 4C_{55}) \\ 2(C_{11} + 8C_{12} + C_{22} + 5C_{23} - 4C_{55}) & 2(3C_{11} + 4C_{12} + 8C_{22} + 8C_{55}) & 2(C_{11} + 8C_{12} + C_{22} + 5C_{23} - 4C_{55}) \\ 2(C_{11} + 8C_{12} + C_{22} + 5C_{23} - 4C_{55}) & 2(C_{11} + 8C_{12} + C_{22} + 5C_{23} - 4C_{55}) & 2(3C_{11} + 4C_{12} + 8C_{22} + 8C_{55}) \\ 0 & 0 & 0 \\ 0 & 0 & 0 \\ 0 & 0 & 0 \\ 0 & 0 & 0 \\ 0 & 0 & 0 \\ 0 & 0 & 0 \\ (2C_{11} - 4C_{12} + 7C_{22} - 5C_{23} + 12C_{55}) & 0 & 0 \\ 0 & (2C_{11} - 4C_{12} + 7C_{22} - 5C_{23} + 12C_{55}) & 0 \\ 0 & 0 & (2C_{11} - 4C_{12} + 7C_{22} - 5C_{23} + 12C_{55}) \end{bmatrix}, \end{aligned}$$

analytical rather than numerical methods. In each case it was noted that extension of the relevant equations was probably unfeasible without closer scrutiny of the particular curve shapes, and introduction of significant simplifications. The process is analogous to determination of empirical equations from experimental data. Instead of physical experimentation, however, a kind of numerical experiment is performed from which an empirical relation is deduced. It is the authors' belief that consideration of this process, while simple in

where $C_{\alpha\beta}$ refers to the (α, β) term of the fibre sub-unit stiffness matrix in local, fibre aligned coordinates—refer to Ault and Hoffman (1992). A similar result was obtained by Christensen and Waals (1972), who noted that the above matrix is in fact isotropic. Each $C_{\alpha\beta}$ is a function of fibre and matrix phase shear moduli (G_f and G_m , respectively) and Poisson ratios (ν_f and ν_m , respectively), and fibre volume fraction, V_f . Since \bar{C}_{ij} is isotropic, we have $\bar{G} = \bar{C}_{44} = \Phi(G_f, G_m, \nu_f, \nu_m, V_f)$. Holding all other variables constant and expressing \bar{G}

in terms of G_m only, an expression of the form

$$\tilde{G} = \frac{a_0 + a_1 G_m + a_2 G_m^2 + a_3 G_m^3 + a_4 G_m^4}{b_0 + b_1 G_m + b_2 G_m^2 + b_3 G_m^3}$$

is obtained, where a_i and b_i are constants.

References

Ault, H.K., Hoffman, A.H., 1992. A composite micromechanical model for connective tissues: part I—theory. *Journal of Biomechanical Engineering* 114, 137–141.

Christensen, R.M., Waals, F.M., 1972. Effective stiffness of randomly oriented fibre composites. *Journal of Composite Materials* 6, 518–532.

Germanovich, L.N., Dyskin, A.V., 1994. Virial expansions in problems of effective characteristics. 1. General concepts. *Mechanics of Composite Materials* 30/2, 222–237 (in Russian).

Hashin, Z., Rosen, B.W., 1964. The elastic moduli of fiber-reinforced materials. *Journal of Applied Mechanics* 31, 223–232.

Miller, K., 2001. How to test very soft biological tissues in extension? *Journal of Biomechanics* 34, 651–657.

Miller, K., 2004. Method of testing very soft biological tissues in compression. *Journal of Biomechanics*, in press, available from www.sciencedirect.com.

Schwartz, M.H., Leo, P.H., Lewis, J.L., 1994. A microstructural model for the elastic response of articular cartilage. *Journal of Biomechanics* 27, 865–873.

Simha, N.K., Fedewa, M., Leo, P.H., Lewis, J.L., Oegema, T., 1999. A composites theory predicts the dependence of stiffness of cartilage culture tissues on collagen volume fraction. *Journal of Biomechanics* 32, 503–509.

Wilson, W., van Donkelaar, C.C., van Rietbergen, B., Ito, K., Huiskes, R., 2004. Stresses in the local collagen network of articular cartilage: a poroviscoelastic fibril-reinforced finite element study. *Journal of Biomechanics* 37, 357–366.